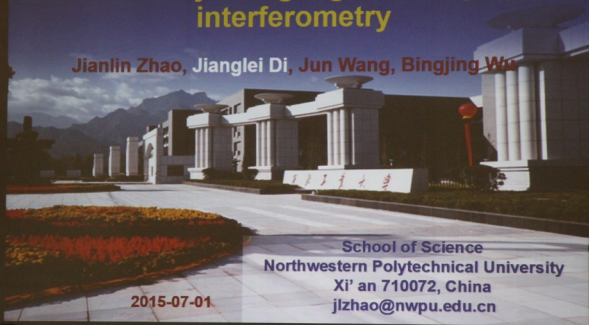


ISDH2015, June, St Petersburg, Russia

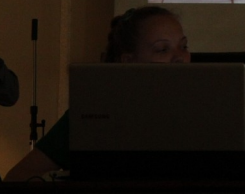
Display and measurement of complex flow fields by using digital holographic interferometry

Jianlin Zhao, Jianglei Di, Jun Wang, Bingjing Wu



School of Science
Northwestern Polytechnical University
Xi'an 710072, China
jlzhao@nwpu.edu.cn

2015-07-01





Complex flow field



Airflow and temperature induced by flame



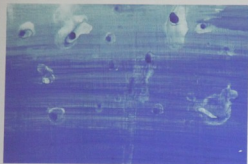
Atmospheric Motion



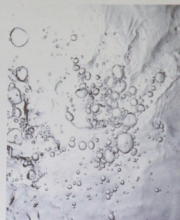
Airflow in wind tunnel



Complex flow field

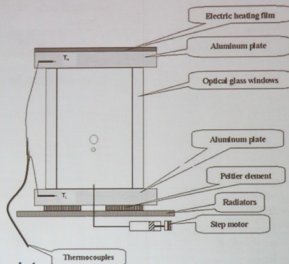


Liquid diffusion



Bubbles motion

Complex flow field



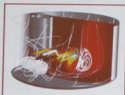
The motion of double droplets



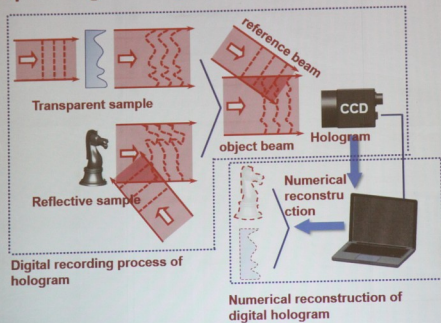
Introduction

6

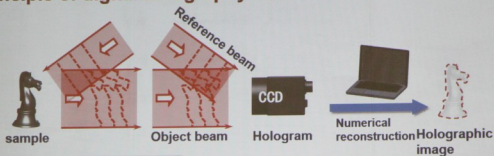
How to achieve the visual, dynamical, non-destructive, high precision, full-field, quantitative measurement and display for complex flow field?



Principle of digital holography



Principle of digital holography



$$O(x, y) = O_0(x, y) \exp[i\phi_0(x, y)]$$

$$R(x, y) = R_0(x, y) \exp[i\phi_R(x, y)]$$

$$I(x, y) = |O(x, y) + R(x, y)|^2$$

$$= O_0^2(x, y) + R_0^2(x, y)$$

$$+ 2O_0(x, y)R_0(x, y) \cos[\phi_0(x, y) - \phi_R(x, y)]$$

$$U(\xi, \eta) = -\frac{i}{\lambda d} \exp\left(i\frac{2\pi}{\lambda}d\right) \exp[i\pi\lambda d(v^2 + \mu^2)]$$

$$\times F\left\{R(x, y) \exp\left[i\frac{\pi}{\lambda d}(x^2 + y^2)\right]\right\}$$

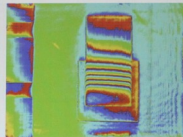
Principle of digital holography

Holographic image intensity

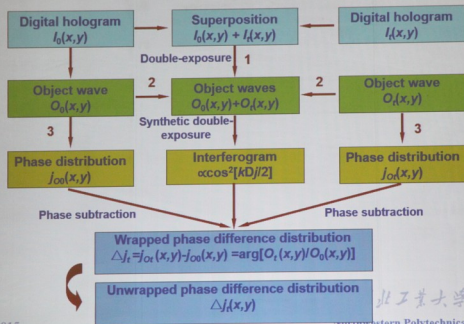
$$I(\xi, \eta) = |U(\xi, \eta)|^2$$

Holographic image phase

$$\varphi(\xi, \eta) = \arctan \frac{\text{Im}[U(\xi, \eta)]}{\text{Re}[U(\xi, \eta)]}$$



Principle of digital holographic interferometry (DHI)



Relationship of phase difference and flow fields

Distribution of refractive index change

Assuming that the index of flow field along the optical path (z axis) is uniform, the relationship between the index and phase changes can be expressed as

$$\Delta\varphi_t(x, y) = \frac{\lambda}{2\pi} (n_t(x, y) - n_0) d(x, y) = \frac{\lambda}{2\pi} \Delta n(x, y) d(x, y)$$

Then we can obtain the index change distribution

$$\Delta n(x, y) = \frac{2\pi}{\lambda} \cdot \frac{\Delta\varphi_t(x, y)}{d(x, y)}$$

Relationship of phase difference and flow fields

Solution concentration

The relationship between the index change and the solution concentration

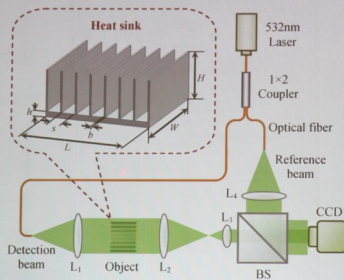
$$\Delta n(x, y) = \left[\frac{\partial n_z}{\partial T} \right]_c [T_i(x, y) - T_0(x, y)] + \left[\frac{\partial n_z}{\partial C} \right]_T [C_i(x, y) - C_0(x, y)]$$

Under the condition of constant temperature, we have

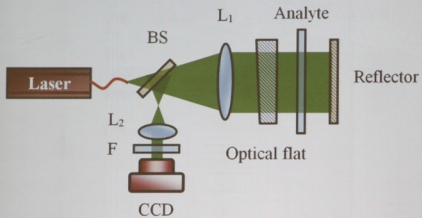
$$C_i(x, y) = C_0(x, y) + \left\{ \frac{\lambda}{2\pi d(x, y)} \Delta \varphi_i(x, y) \right\} \left/ \left[\frac{\partial n_z}{\partial C} \right]_T \right.$$

Similar ways can be used to obtain the distributions of temperature, density, velocity, as well as diffusion coefficient of flow fields.

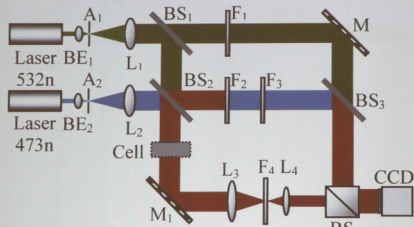
Experimental setup based on Mach-Zehnder interferometer



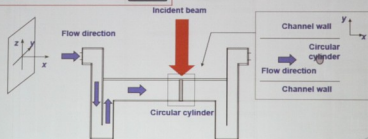
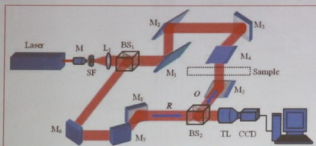
Experimental setup based on Fizeau interferometer



Experimental setup based on Mach-Zehnder interferometer with dual-wavelength technique



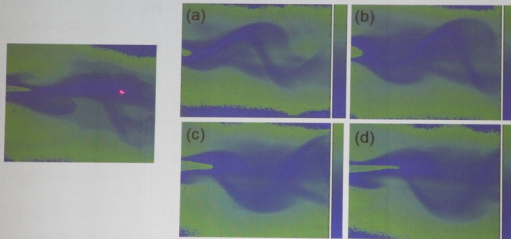
Application 1: Karman vortex street in water flow field



Sample for Karman vortex street generation

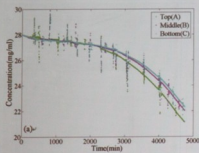


Application 1: Phase difference distribution of Karman vortex street

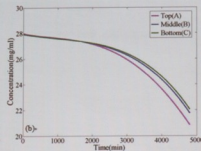


Application 2: Crystallization process in protein-lysozyme solution

Solution concentration variation plots during crystallization process



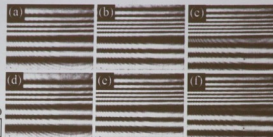
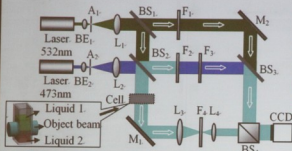
Measurement results of the solution concentration in the top, middle, bottom regions;



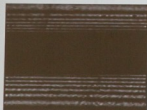
Fitting results corresponding to (a)



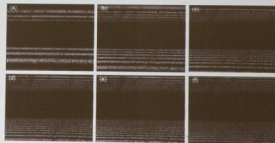
Application 3: Liquid diffusion



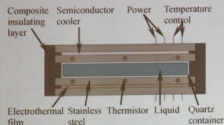
Ternary diffusion process in liquids



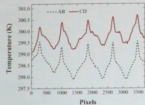
Diffusion process between water and alcohol



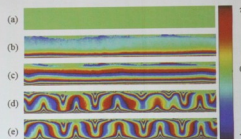
Application 4: Rayleigh-Benard convection (RBC)



Temperature distribution at horizontal positions



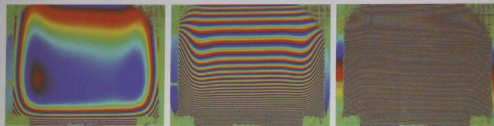
Phase difference of RBC



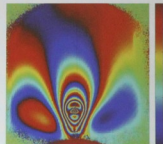
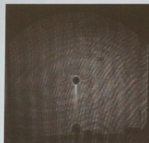
(a) 0s; (b) 20s; (c) 42s; (d) 86s; (e) 133s



Application 5: Thermocapillarity of droplets



Phase difference of temperature field in liquid container



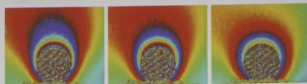
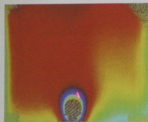
J. D. Li, S. Kang, et al, *DH2015*. 2015, 5



Application 5

25

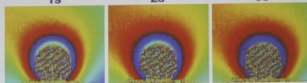
Application 5: Suspended and motion state of droplet



1s

2s

5s



7s

9s

11s



45s

65s

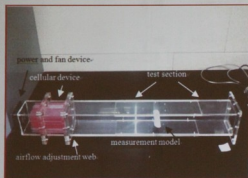
85s

ISIJ, D. M. Li, S. Kang, et al, DH2015, 2015, 5

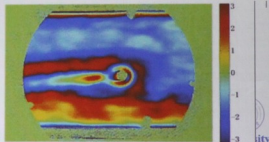
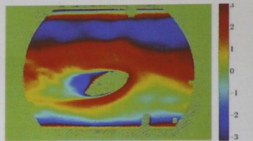
Northwestern Polytechnical University



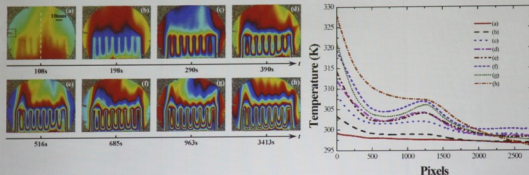
Application 6: Air flow in wind tunnel



Wind tunnel model

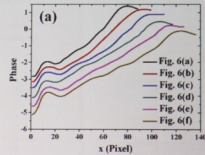
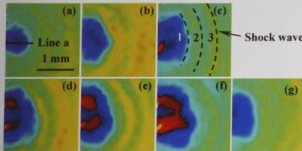
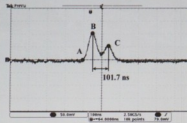
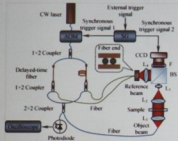


Application 7: Heat exchange process of air flow field near heat sink

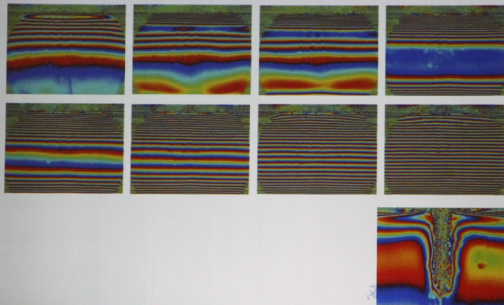


Temperature distributions along the vertical direction in (a)-(h)

Application 8: Shockwave field

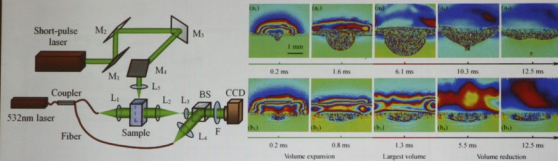


Application 9: Unstable reaction-diffusion process



Application 10: Laser ablation on the surfaces of liquid

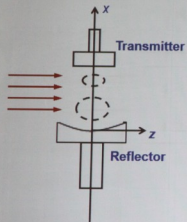
Phase difference distributions of the ablation region



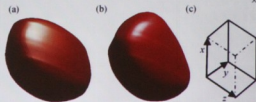
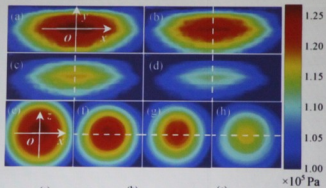
(a) Deionized water using 470 mJ energy; (b) glycerin using 470 mJ energy.

From the phase change between the two adjacent pixels in saltation process, the boundaries of cavity and jet can be detected.

Application 11: Ultrasonic standing wave



Ultrasonic standing wave device





Summary

33

- Several applications of digital holographic interferometry in display and measurement of complex flow fields are presented.
- Related experiment results with specially designed setups during the dynamic evolution processes of flow fields are shown.
- Digital holographic interferometry is an effective tool.

